

ACCEPTED MANUSCRIPT • OPEN ACCESS

Electron collision studies on the CH₂⁺ molecular ion

To cite this article before publication: Kalyan Chakrabarti *et al* 2022 *J. Phys. B: At. Mol. Opt. Phys.* in press <https://doi.org/10.1088/1361-6455/ac4ff2>

Manuscript version: Accepted Manuscript

Accepted Manuscript is “the version of the article accepted for publication including all changes made as a result of the peer review process, and which may also include the addition to the article by IOP Publishing of a header, an article ID, a cover sheet and/or an ‘Accepted Manuscript’ watermark, but excluding any other editing, typesetting or other changes made by IOP Publishing and/or its licensors”

This Accepted Manuscript is © 2022 The Author(s). Published by IOP Publishing Ltd..

As the Version of Record of this article is going to be / has been published on a gold open access basis under a CC BY 3.0 licence, this Accepted Manuscript is available for reuse under a CC BY 3.0 licence immediately.

Everyone is permitted to use all or part of the original content in this article, provided that they adhere to all the terms of the licence <https://creativecommons.org/licenses/by/3.0>

Although reasonable endeavours have been taken to obtain all necessary permissions from third parties to include their copyrighted content within this article, their full citation and copyright line may not be present in this Accepted Manuscript version. Before using any content from this article, please refer to the Version of Record on IOPscience once published for full citation and copyright details, as permissions may be required. All third party content is fully copyright protected and is not published on a gold open access basis under a CC BY licence, unless that is specifically stated in the figure caption in the Version of Record.

View the [article online](#) for updates and enhancements.

Electron collision studies on the CH_2^+ molecular ion

K. Chakrabarti¹, J. Zs. Mezei^{2,3}, I. F. Schneider³ and J. Tennyson^{4,3}

¹Department of Mathematics, Scottish Church College, 1 & 3-Urquhart Sq., Kolkata 700006, India

²Institute for Nuclear Research, 4001 Debrecen, Hungary

³LOMC-UMR6294 CNRS-Université Le Havre Normandie, 76058 Le Havre, France

⁴Department of Physics and Astronomy, University College London, Gower St., London WC1E 6BT, UK

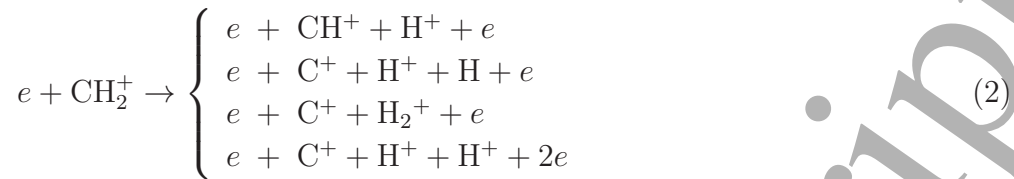
Abstract. Calculations are performed for electron collision with the methylene molecular ion CH_2^+ in its bent equilibrium geometry, with the goal to obtain cross sections for electron impact excitation and dissociation. The polyatomic version of the UK molecular *R*-matrix codes was used to perform an initial configuration-interaction calculation on the doublet and quartet states of the CH_2^+ ion. Subsequently, scattering calculations are performed to obtain electron impact electronic excitation and dissociation cross sections and, additionally, the bound states of the CH_2 molecule and Feshbach resonances in the $e\text{-CH}_2^+$ system.

1. Introduction

Many low temperature plasma environments have hydrocarbon molecular ions as important constituents. Collision of electrons with molecules and their ions in these environments are important processes that play a fundamental role in initiating chemistry, particle balance and transport. For example, although the present tendency in the magnetically controlled International Thermonuclear Fusion Reactor (ITER) type fusion devices is to coat the reactor walls with beryllium or tungsten, hydrocarbon ions, in particular the methylene ion CH_2^+ , are found in the edge and divertor plasmas of fusion devices which operate with graphite as plasma facing material (McLean et al. 2005). Another important context is that of the dusty plasmas, the CH_2 and CH_2^+ being species involved in the chain of reactions resulting in the growths of the nano and micro-particles. In these situations, the cross sections for different electron induced process are necessary to model the plasma flow (see for example Reiter & Janev (2010)), in particular electron impact dissociation and dissociative ionisation:



1
2
3 *e-CH₂⁺ collisions*



9
10 These processes, leading to the destruction of the CH₂⁺ ions and to the C atom
11 production (Janev & Reiter 2002*a*, Janev & Reiter 2002*b*), are highly significant for
12 understanding the carbon redeposition.
13

14 In the interstellar medium (ISM), CH₂⁺ ions are synthesised in gas phase by collision
15 of C⁺ ions with hydrogen (Wakelam et al. 2010) and through hydrogen abstraction by
16 CH⁺. On the other hand, CH₂⁺ ions can be removed by reactions such as (1), (2) and
17 by dissociative recombination (DR),
18



23 which is known to proceed via Feshbach resonances (Larson et al. 1998).
24

25 There is a considerable literature on CH_y⁺ hydrocarbon ions, and CH₂⁺ ions in
26 particular, in the context of synthesis of hydrocarbons in the ISM (van Dishoeck
27 et al. 1996, van Dishoeck et al. 2006, Wakelam et al. 2010, Puglisi et al. 2018, IdBarkach
28 et al. 2019). Significant work on CH_y⁺ hydrocarbon ions have also been done
29 relevant to plasmas for fusion (Janev & Reiter 2002*a*, Janev & Reiter 2002*b*, Vane
30 et al. 2007, Lecointre et al. 2009, Reiter & Janev 2010). These works mainly focus on
31 different electron impact cross sections relevant for plasma modeling.
32

33 Molecular structure calculations on CH₂⁺ have been reported by several authors
34 (Tennyson & Sutcliffe 1983, Theodorakopoulos & Petsalakis 1991, Kraemer et al. 1994,
35 Li et al. 2015, Guo et al. 2018, Ma et al. 2021). Theodorakopoulos & Petsalakis (1991)
36 obtained bending potential energy curves (PEC) and vertical excitation energies of CH₂⁺
37 for its bent *C_{2v}* and its linear *D_{∞h}* configurations. Accurate global potential energy
38 surfaces (PES) were reported by Li et al. (2015) and Guo et al. (2018). Apart from these,
39 there are also many spectroscopic studies on the rovibrational states of CH₂⁺ (Rösslein
40 et al. 1992, Bunker et al. 2001, Jensen et al. 2002, Willitsch & Merkt 2003, Wang
41 et al. 2013).
42

43 In a number of earlier studies (Chakrabarti et al. 2017, Chakrabarti et al. 2018,
44 Chakrabarti et al. 2019, Ghosh et al. 2020) we have studied electron collision with the
45 CH molecule and its positive ion CH⁺ in considerable detail. In these works, we not
46 only computed cross sections for different electronic processes, but also identified many
47 new neutral valence states of CH that are relevant for the DR. The present article aims
48 to continue and extend our work to more complex hydrocarbon ions.
49
50
51
52
53
54
55
56
57
58
59
60

1
2
3 *e-CH₂⁺ collisions*

3

4 **2. R-matrix Calculations**

6 *2.1. R-matrix method*

8
9 The *R*-matrix method, described in detail by Tennyson (2010) and Burke (2011), and
10 its implementation in the polyatomic version of the UK molecular *R*-matrix codes
11 (UKRmol) (Carr et al. 2012) is used in the present work. The method employs a division
12 of space into an inner region, a sphere of radius a (chosen to be $10 a_0$ in this work) called
13 the *R*-matrix sphere whose purpose is to include within it all short range interactions,
14 and an outer region exterior to this sphere which contains all the long range interactions.
15 This division allows the treatment of the short range and, the more complicated, long
16 range interactions separately using different techniques (Tennyson 2010).
17

18
19 In the inner region, the wave function of the target (here CH₂⁺) and a single
20 continuum electron, together having $N + 1$ electrons, is taken as

$$21 \Psi_k = \mathcal{A} \sum_{i,j} a_{i,j,k} \Phi_i(1, \dots, N) F_{i,j}(N+1) + \sum_i b_{i,k} \chi_i(1, \dots, N+1), \quad (4)$$

22
23 where \mathcal{A} is an antisymmetrisation operator, $\Phi_i(1, \dots, N)$ is the wave function of the N
24 electron target and $F_{i,j}(N+1)$ are continuum orbitals. The functions $\chi_i(1, \dots, N+1)$
25 in the last term are square integrable functions, called L^2 functions, are constructed
26 by allowing the projectile electron to enter the target complete active space (CAS) and
27 are included to take into account electron correlations and polarization of the target
28 in presence of the projectile electrons. The coefficients $a_{i,j,k}$ and $b_{i,k}$ are obtained by
29 diagonalizing the inner region Hamiltonian (Tennyson 1996).
30

31
32 The inner region wave function Ψ_k is then used with appropriate boundary
33 conditions to obtain scattering information, the details of which are given in the following
34 subsections.
35

36 *2.2. Target calculations*

37
38 We used the cc-pVTZ Gaussian basis sets (Pritchard et al. 2019) centered on the C
39 and H atoms to represent the target orbitals. These not only gave reasonably good
40 target vertical excitation energies but also allows the inner region calculation to remain
41 manageable with respect to computational resources.

42
43 The X ²A₁ ground state of CH₂⁺ is known to be bent in C_{2v} symmetry and has
44 the electronic configuration (1a₁)²(2a₁)²(1b₂)²(3a₁)¹ (Pople & Curtiss 1987, Graber
45 et al. 1993). In this work all calculations are reported at the equilibrium C-H bond
46 length 2.066 a₀ and the H-C-H bond angle 140.1° taken from Theodorakopoulos &
47 Petsalakis (1991), which are very close to those obtained by more sophisticated coupled
48 cluster calculations using large basis sets (Brinkmann et al. 2002). An initial Hartree-
49 Fock (HF) calculation was first performed on the X ²A₁ ground state of CH₂⁺. The HF
50 orbitals were then used in a configuration interaction (CI) calculation.
51

52
53 We considered two target models. In both models we kept two electrons frozen in the
54 1a₁ orbitals while the remaining five electrons were distributed in the CAS. In the first
55
56
57
58
59
60

e-CH₂⁺ collisions

model (M1), the complete active space was defined by $(1a_1 - 6a_1, 1b_1 - 4b_1, 1b_2 - 4b_2)$, while in the second (M2) the CAS was chosen to be bigger with an additional $1a_2$ orbital, namely $(1a_1 - 8a_1, 1b_1 - 5b_1, 1b_2 - 5b_2, 1a_2)$. Table 1 shows the comparison of the vertical excitation energies (VEE) from the X 2A_1 ground state of CH₂⁺ to the first 12 low lying excited states. Although the second model M2 appears to produce VEEs slightly in better agreement with the theoretical results of Theodorakopoulos & Petsalakis (1991) and Osmann et al. (1999), calculations with this model required much longer time compared to the model M1. We therefore chose the model M1 for subsequent calculations as it was computationally more efficient.

From Table 1, we see that apart from the VEE of the 4^2A_1 state, which appears too high compared to Theodorakopoulos & Petsalakis (1991), all other vertical excitation energies obtained by the target model M1 are in reasonably good agreement with the results of Theodorakopoulos & Petsalakis (1991) and Osmann et al. (1999). Moreover, our dipole moment for the CH₂⁺ ground state with model M1 is 0.701 D which compares perfectly with the value 0.701 D obtained by Brinkmann et al. (2002) using coupled cluster calculation. The model M1 therefore provides a good description of the target for subsequent scattering calculations.

2.3. Scattering calculations

For the scattering calculations, we used 8 a_1 , 6 b_1 , 6 b_2 and 2 a_2 target orbitals allowing 2 virtual orbitals for each symmetry. Since the target CH₂⁺ is a positive ion, the continuum functions were represented by Coulomb functions which were obtained as a solution of the radial Coulomb equation for an isotropic Coulomb potential, and the solutions with $l \leq 4$, and energy eigenvalue ≤ 5 Ryd were retained in the calculation. The Coulomb functions were then fitted to GTOs using the procedure outlined in Faure et al. (2002).

The target and continuum orbitals must all be orthogonal to each other. To ensure the orthogonality, the target and continuum orbitals were first individually Schmidt orthogonalized and finally the full set of target and continuum orbitals were symmetric orthogonalized, retaining only those orbitals for which the eigenvalue of their overlap matrix was less than a deletion threshold, chosen here to be 5×10^{-5} . The deletion threshold depends on the R -matrix radius and was adjusted to ensure that there was no linear dependence.

An R -matrix was built at the boundary of the inner and outer region from the inner region solutions (Eq.(4)). The R -matrix were then propagated to an asymptotic distance $R_{asy} = 70 a_0$ in a potential which included the Coulomb potential and the dipole and quadrupole potentials of the target, where they were then matched to asymptotic functions obtained from a Gailitis expansion (Noble & Nesbet 1984). This matching procedure yields the K -matrix from which all scattering observables can be obtained. A different route, however, is followed for obtaining bound states, as is outlined below.

For bound states, the R -matrix and wave functions were propagated using Runge-Kutta-Nystrom method (Zhang et al. 2011) to an asymptotic distance $R_{asy} = 50 a_0$

$e\text{-CH}_2^+$ collisions

5

Table 1: Comparison of the vertical excitation energies (in eV) from the X 2A_1 ground state to 12 low lying excited states of CH_2^+ for different target models. The target models used are the following:

M1: $(1a_1)^2(1a_1 - 6a_1, 1b_1 - 4b_1, 1b_2 - 4b_2)^5$

M2: $(1a_1)^2(1a_1 - 8a_1, 1b_1 - 5b_1, 1b_2 - 5b_2, 1a_2)^5$

| Target state | M1 | M2 | Theory ^a | Theory ^b |
|--------------|----------------|----------------|---------------------|---------------------|
| X 2A_1 | 0 ^c | 0 ^d | 0 ^e | 0 |
| 1 2B_1 | 0.92 | 0.81 | 0.84 | 0.83 |
| 1 4A_2 | 5.24 | 5.07 | | |
| 1 2A_2 | 6.93 | 6.81 | 6.81 | 6.92 |
| 1 2B_2 | 7.46 | 7.36 | 7.60 | 7.8 |
| 2 2A_2 | 7.88 | 7.60 | 7.25 | 7.26 |
| 1 4B_1 | 9.73 | 9.58 | | |
| 2 2B_2 | 9.48 | 9.17 | 9.25 | 9.6 |
| 2 2A_1 | 11.17 | 10.50 | 10.44 | 11.1 |
| 3 2A_1 | 13.52 | 13.04 | 12.81 | |
| 2 2B_1 | 13.47 | 13.21 | 13.14 | 13.9 |
| 4 2A_1 | 14.89 | 14.76 | 13.40 | |
| 3 2B_2 | 13.22 | 13.23 | 13.53 | |

^aTheodorakopoulos & Petsalakis (1991)

^bOsmann et al. (1999)

^cAbsolute energy -38.61306904 Hartree

^dAbsolute energy -38.63754516 Hartree

^eAbsolute energy -38.705744 Hartree

in a potential which included the Coulomb potential and the dipole and quadrupole potentials of target, and were matched to exponentially decreasing asymptotic functions (Noble & Nesbet 1984). A searching algorithm (Sarpal et al. 1991) over a non-linear quantum defect based grid (Rabadán & Tennyson 1996) was then used to find the bound states as roots of a determinant $\mathcal{B}(E)$ dependent on the energy. The details of the method are omitted and can be found in Sarpal et al. (1991).

3. Results

All scattering calculations in this work were performed at a single geometry, namely the equilibrium geometry of the CH_2^+ target ion, for bound states of the CH_2 molecule, Feshbach resonances in the $e+\text{CH}_2^+$ system and cross sections for elastic scattering and electronic excitations. An 11 state scattering model including three 2A_1 , three 2B_1 , three 2B_1 and two 2A_2 target states in the close coupling expansion Eq. (4) were used for the singlet $e+\text{CH}_2^+$ scattering close-coupling expansion, while a 15 state model which included the same 11 doublet states as in the singlet state model,

1
2
3 *e-CH₂⁺ collisions* 6

4 together with the lowest each of the ⁴A₁, ⁴B₁, ⁴B₂, and ⁴A₂ states was used in Eq. (4)
5 for triplet symmetry close-coupling expansion. As will be shown below, this procedure
6 provides a reliable scattering model which was tested by calculating the bound states
7 of CH₂.
8
9

10
11 *3.1. Bound states*

12
13 Table 2 shows the vertical excitation energies for the bound states of CH₂ from its
14 X ³B₁ ground state to few of its low lying excited states. For a comparison, we also did
15 a quantum chemistry-style CI calculation on CH₂ at its equilibrium geometry (C-H bond
16 length 2.0314 a₀ and H-C-H bond angle 133.8°) using a (1a₁)²(2 - 6a₁, 1 - 4b₁, 1 - 4b₂)⁶
17 CAS-CI model. The vertical excitation energies are then compared with the multi
18 reference double excitation (MRD-CI) calculation of Römelt & Peyerimhoff (1981) and
19 the coupled cluster results of Yamaguchi & Shaeffer III (1997). From Table 2, it is
20 clear that the vertical excitation energies obtained by the *R*-matrix method are in very
21 good agreement with all others. The fact that the calculated bound state energies are
22 consistent and accurate enough indicates that our scattering model is reasonably good.
23
24
25
26
27
28
29

30 Table 2: Comparison of the vertical excitation energies (in eV) from the ground X ³B₁
31 state of CH₂ to some of its low lying excited states.

| CH ₂ state | This work | CI ^a | Romelt ^b | Yamaguchi ^c |
|-------------------------------|------------------|------------------|---------------------|------------------------|
| X ³ B ₁ | 0.0 ^d | 0.0 ^e | 0.0 ^f | 0.0 |
| 1 ¹ A ₁ | 1.16 | 0.995 | 1.14 | |
| ¹ B ₁ | 1.74 | 1.86 | 1.63 | |
| 2 ¹ A ₁ | 3.24 | 3.31 | 3.38 | |
| ³ A ₁ | 6.21 | 7.67 | 6.37 | |
| ³ B ₂ | 7.35 | 8.05 | 7.59 | 7.86 |
| ¹ B ₂ | 7.25 | 9.25 | 7.63 | 7.75 |
| ³ A ₂ | 7.63 | 7.47 | 7.57 | 7.23 |
| ¹ A ₂ | 8.33 | 8.39 | 8.46 | |

32
33
34
35
36
37
38
39
40
41
42
43
44
45
46 ^aCI calculation done at CH₂ equilibrium (C-H bond length 2.0314 a₀ and H-C-H bond
47 angle 133.8°) using (1a₁)²(2a₁ - 6a₁, 1b₁ - 4b₁, 1b₂ - 4b₂)⁶ CAS-CI model.

48 ^bRömelt & Peyerimhoff (1981)

49 ^cYamaguchi & Shaeffer III (1997)

50
51 ^{d,e,f} Absolute energies of the ground states are respectively -38.985233^d Hartree,
52 -38.966950^e Hartree and -39.06034^f Hartree.
53
54
55
56
57
58
59
60

e-CH₂⁺ collisions

7

3.2. Resonances at equilibrium

For resonance calculation, the R -matrix was propagated to $70 a_0$. Resonances were detected by the characteristic change in sign of the second derivative of the eigenphase sum $\delta(E)$ given by

$$\delta(E) = \sum_i \arctan(K_{ii}), \quad (5)$$

where K_{ii} are the diagonal elements of the K matrix. They were then fitted to a Breit-Wigner profile (Tennyson & Noble 1984) with an energy grid 0.005 eV to obtain the resonance energy E and width Γ .

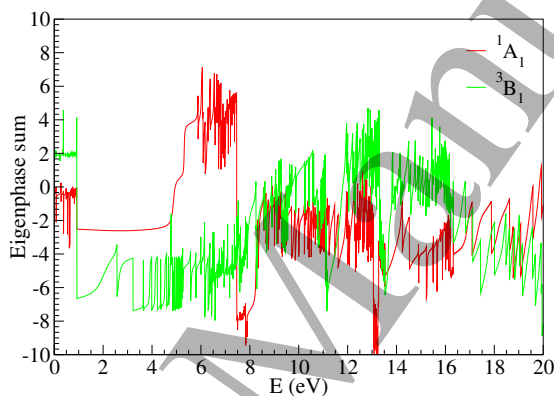


Figure 1: Eigenphase sums for the overall $e + \text{CH}_2^+$ symmetries 1A_1 and 3B_1 .

Figure 1 shows the plot of two typical eigenphase sums for 1A_1 and 3B_1 symmetries. Characteristic of electron collision with ions, the figure shows numerous resonances some of which are tabulated in Table 3 according to their parent state. As seen from the table, many of the resonances appear to be in Rydberg series which can be identified by their effective quantum numbers. The relatively small gap between the ground and first excited electronic state means that the resonances start with relatively high effective quantum numbers, $\nu \approx 4$, and then closely space.

A full set of fits to the resonances covering all overall scattering symmetries is given in the supplementary material.

3.3. Electron impact excitation

Our calculated cross sections for electron impact excitation of CH_2^+ from the ground state to four of its lowest doublet states are shown in Figure 2. As in the elastic cross section, the excitation cross sections show highly resonant behaviour due to temporary captures into resonant states. Particularly, the $X \ ^2A_1 \rightarrow 1 \ ^2B_1$ excitation cross section shows evidence of a large resonance near threshold. Referring to Figure 1, this is likely due to the large 3B_1 resonance near 1 eV as seen from the plot of the 3B_1 eigenphase

$e\text{-CH}_2^+$ collisions

Table 3: Resonance positions and widths (in Ryd) and effective quantum numbers at the CH_2^+ equilibrium for states of 3B_1 and 1A_1 symmetry of the $e\text{-CH}_2^+$ system below the first two CH_2^+ excited states. Numbers within brackets indicate power of 10.

| Position | Width | ν | Position | Width | ν |
|----------------------|-------------|--------|----------------------|-------------|--------|
| 3B_1 symmetry | | | | | |
| Below 1^2B_1 state | | | Below 4A_2 state | | |
| 0.3558(-02) | 0.2400(-04) | 3.9466 | 0.1925 | 0.1075(-01) | 2.2792 |
| 0.4870(-02) | 0.5833(-04) | 3.9875 | 0.2678 | 0.3334(-03) | 2.9201 |
| 0.1567(-01) | 0.4765(-04) | 4.3815 | 0.2872 | 0.2789(-02) | 3.1980 |
| 0.1718(-01) | 0.6172(-04) | 4.4465 | 0.3034 | 0.1910(-03) | 3.5000 |
| 0.2685(-01) | 0.1503(-04) | 4.9440 | 0.3197 | 0.2426(-03) | 3.9143 |
| 1A_1 symmetry | | | | | |
| Below 1^2B_1 state | | | Below 1^2A_2 state | | |
| 0.2034(-01) | 0.2198(-03) | 4.5925 | 0.3582 | 0.9116(-02) | 2.5716 |
| 0.3582(-01) | 0.1225(-03) | 5.5953 | 0.3907 | 0.2355(-02) | 2.9015 |
| 0.4478(-01) | 0.7510(-04) | 6.5969 | 0.4323 | 0.1280(-02) | 3.6009 |
| 0.5043(-01) | 0.4929(-04) | 7.5979 | 0.4424 | 0.2339(-02) | 3.8615 |
| 0.5423(-01) | 0.3407(-04) | 8.5985 | 0.4492 | 0.3074(-02) | 4.0762 |

sum. Generally, the excitation cross sections decrease with increasing incident energy and the cross sections from the higher lying excited states are much smaller.

Our calculations only consider partial waves with $l \leq 4$. For dipole allowed electronic excitation processes it is known that higher l partial waves contribute to the electronic excitation and for electron collisions with neutral targets allowance for this is often made using the Born approximation; a standard procedure exists for this within the UKRMol codes (Kaur et al. 2008). Considering the low-lying states of CH_2^+ excitation the two low-lying 2A_2 states are dipole forbidden but the 1^2B_1 and 1^2B_2 are both connected to the ground state by dipoles in the region of 1 a.u. Test calculations showed that allowing for this approximately led to a small increase in the 1^2B_2 cross section but a very large increase in the predicted electronic excitation cross section for the 1^2B_1 . However, the 1^2B_1 state has a very low excitation threshold meaning it will be excited by slow-moving electrons and that under these circumstances it is necessary to consider the rotational motion of the target which will lead a reduction in effect of the long-range dipole. Treatment of this will require further developments and is left to future work. However, neglect of the partial waves with $l > 4$ means that our predicted 1^2B_1 and 1^2B_2 cross sections, and the dissociation cross sections given below, are probably too low.

$e\text{-CH}_2^+$ collisions

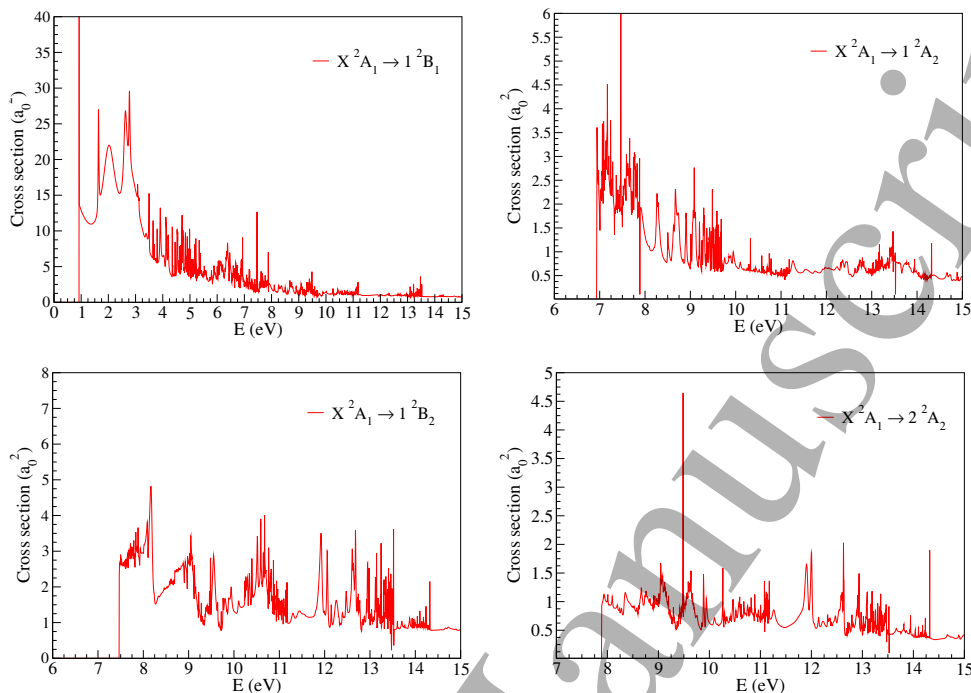


Figure 2: Cross sections for electronic excitation from the X^2A_1 ground state to the first four excited states of doublet symmetry as given in Table 1 and indicated in each panel.

3.4. Electron impact dissociation

Experimental cross sections for electron impact dissociation were obtained by Vane et al. (2007) for the production of CH^+ and C^+ fragments. Although model calculations exist for the electron impact dissociation of CH_2^+ ions (see for example Reiter & Janev (2010)), to the best of our knowledge, the 2007 experiments have never been described by any *ab initio* calculation.

The dissociation of CH_2^+ into the lowest dissociation channels, namely $e + \text{CH}^ + \text{H}$ and $e + \text{C}^ + \text{H}_2$, proceed via direct dissociative excitation and have thresholds 6.08 eV and 5.62 eV respectively (Vane et al. 2007). In deriving the dissociation cross section, we assumed that electronic excitations to all states above the respective dissociation thresholds lead to dissociation. In our calculation, we have included the states 1^2B_1 , 1^2B_2 , 1^2A_2 , and the 2^2A_2 excited states all of which lie close to one another at the CH_2^+ equilibrium. Moreover, except the 1^2B_1 state, which has both valence and Rydberg character, all the other three are of valence character at equilibrium (see for example (Theodorakopoulos & Petsalakis 1991)) and hence are likely to dissociate to the $e + \text{C}^ + \text{H}_2$ (5.62 eV) or the $e + \text{CH}^ + \text{H}$ (6.08 eV) dissociation limits, which are the most relevant in the energy range considered. Since the dissociation channels cannot be separated in our calculations, our cross section in Figure 3 represents a sum over these channels. For better comparison, we have also shown our cross sections after smoothing

$e\text{-CH}_2^+$ collisions

10

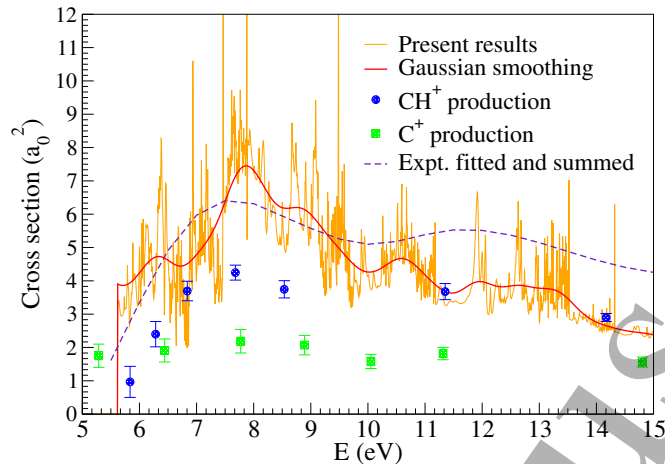


Figure 3: Cross section for the electron impact dissociation of the CH_2^+ ion. Thin curve: present R -matrix results (see text). Thick (red) curve: present result after smoothing with a Gaussian function. Green circles with error bars: experimental results for C^+ ion production Vane et al. (2007). Blue circles with error bars: experimental results for CH^+ ion production Vane et al. (2007). Dashed curve: experimental results for C^+ and CH^+ ion production summed after suitable fitting (see text).

by using a Gaussian function. The experimental data from Vane et al. (2007) are available for each of the dissociation channels mentioned above. The energy grid of the experimental cross sections for these two dissociation channels, however, are neither same nor uniform. Therefore, to sum the experimental data, we first spline interpolated each set over the same and uniform energy grid. This allowed us to sum the cross section for the experimental data. In Figure 3, this sum is shown as the dashed line and it agrees fairly well with our computed cross section. In particular, the peak near 8 eV agrees quite well with the spline interpolated summed experimental curve. However, we note that since the experimental data is non uniformly spaced, the interpolated curve may not often reflect the actual trend. For example, we suspect the agreement of the interpolated curve with our calculation would have been much better between 11 eV - 15 eV had there been more experimental points available in this region. Similarly, below 6 eV, the interpolated experimental curve appears to diverge for our Gaussian fitted curve. This is a result of the fitting procedure, the interpolated experimental curve actually follows the trend of our raw cross section curve.

4. Conclusion

As mentioned in the introduction, CH_2^+ is a very important constituent in low temperature plasma environments. However, despite its importance, electron collisions studies on CH_2^+ have been rare. In fact, we could not find any *ab initio* calculation for

e-CH₂⁺ collisions

11

the cross sections included in the present work. The only cross section result available, seems to be the total ionisation cross section of CH₂⁺ calculated within the Binary-Encounter-Bethe (BEB) model by Irikura et al. (2002).

In this work, we have presented a reliable set of cross sections for the electronic excitation, and electron impact dissociation of the CH₂⁺ ion. In fact, none of these cross sections have ever been reported before by any *ab initio* calculation. Additionally, we have also calculated and have given the position and width for some of the Feshbach resonances in the e-CH₂⁺ system. These Feshbach resonances, as is well known, are the routes to dissociative recombination of the CH₂⁺ ion. However, its treatment requires a more comprehensive calculation of the resonance energies, widths and the potential energy surfaces of the CH₂⁺ and CH₂ states. This is the subject of an ongoing project.

Data availability

Cross sections and resonance parameters are given as supplementary materials.

Acknowledgements

The authors acknowledge support from Fédération de Recherche Fusion par Confinement Magnétique (CNRS, CEA and Eurofusion), La Région Normandie, FEDER and LabEx EMC3 via the projects PTOLEMEE, Bioengine, the Institute for Energy, Propulsion and Environment (FR-IEPE), and ERASMUS-plus conventions between Université Le Havre Normandie and University College London. We are indebted to Agence Nationale de la Recherche (ANR) via the project MONA, Centre National de la Recherche Scientifique via the Programme National 'Physique et Chimie du Milieu Interstellaire' (PCMI). JZsM thanks the financial support of the National Research, Development and Innovation Fund of Hungary (NKFIH), under the K18 and FK19 funding schemes with project no. K128621 and FK132989. JZsM and IFS are grateful for the support of the NKFIH-2019-2.1.11-TÉT-2020-00100 and Campus France-Programme Hubert Curien-BALATON-46909PM projects.

ORCID iDs

K Chakrabarti <https://orcid.org/0000-0003-0013-5610>

J Zs Mezei <https://orcid.org/0000-0002-7223-5787>

I F Schneider <https://orcid.org/0000-0002-4379-1768>

Jonathan Tennyson <https://orcid.org/0000-0002-4994-5238>

References

- Brinkmann N R, Richardson N A, Wesolowski S S, Yamaguchi Y & Schaefer III H F 2002 *Chem. Phys. Lett.* **352**, 505.
- Bunker P R, Chan M C, Kraemer W P & Jensen P 2001 *Chem. Phys. Lett.* **341**, 358.

$e\text{-CH}_2^+$ collisions

12

- Burke P G 2011 *R-Matrix Theory of Atomic Collisions* Springer-Verlag:Heidelberg.
- Carr J M, Galiatsatos P G, Gorfinkiel J D, Harvey A G, Lysaght M A, Madden D, Mašín Z, Plummer M, Tennyson J & Varambhia H N 2012 *Euro. Phys. J. D* **66**, 58.
- Chakrabarti K, Dora A, Ghosh R, Choudhury B S & Tennyson J 2017 *J. Phys. B: At. Mol. Opt. Phys.* **50**, 175202.
- Chakrabarti K, Ghosh R & Choudhury B S 2019 *J. Phys. B: At. Mol. Opt. Phys.* **52**, 105205.
- Chakrabarti K, Mezei J Z, Motapon O, Faure A, Dulieu O, Hassouni K & Schneider I F 2018 *J. Phys. B: At. Mol. Opt. Phys.* **51**, 104002.
- Faure A, Gorfinkiel J D, Morgan L A & Tennyson J 2002 *Comput. Phys. Commun.* **144**, 224.
- Ghosh R, Chakrabarti K & Choudhury B S 2020 *Plasma Sources Sci. Technol.* **29**, 095016.
- Graber T, Kanter E P, Vager Z & Zajfman Z 1993 *J. Chem. Phys.* **98**, 7725.
- Guo L, Ma H, Zhang L, Song Y & Li Y 2018 *Rsc. Adv.* **8**, 13635.
- Ma H, Zhang C, Song Y, Ma F & Li Y 2021 *J. Phys. Chem. A* **125**, 5490
- IdBarkach T, Chabot M, Béroff K, Negra S D, Lesrel J, Geslin F, Padellec A L, Mahajan T & Díaz-Tendero S 2019 *Astron. Astrophys.* **628**, A75.
- Irikura K K, Kim Y K & Ali M A 2002 *J. Res. Natl. Inst. Stand. Technol.* **107**, 63.
- Janev R K & Reiter D 2002a *Phys. Plasmas* **9**, 4071.
- Janev R K & Reiter D 2002b *Collision Processes of Hydrocarbon Species in Hydrogen Plasmas: I. The Methane Family* (Available from: Forschungszentrum-Jülich, Jülich, Germany).
- Jensen P, Wesolowski S S, Brinkmann N R, Richardson N A, Yamaguchi Y, Schaefer H F & Bunke P 2002 *J. Mol. Spectrosc.* **211**, 257.
- Kaur S, Baluja, K L & Tennyson J 2008 *Phys. Rev. A* **77** 032718.
- Kraemer W P, Jensen P & Bunker P R 1994 *Can. J. Phys.* **72**, 871.
- Larson Å, Padellec A L, Semaniak J, Strömholm C, Larsson M, Rošen S, Peverall R, Danared H, Djuric N, Dunn G H & Datz S 1998 *The Astrophysical Journal* **505**, 459.
- Lecointre J, Belic D S, Jureta J J, K J R & Defrance P 2009 *Euro. Phys. J D* **55**, 569.
- Li Y Q, Zhang P Y & Han K L 2015 *J. Chem. Phys.* **142**, 124302.
- McLean A G, Elder J D, Stangeby P C, Allen S L, Boedo J A, Brooks N H, Fenstermacher M E, Groth M, Lisgo S, Nagy A, Rudakov D L, Wampler W R, Watkins J G, West W P & Whyte D G 2005 *J. Nucl. Materials* **337-339**, 124–128.
- Noble C J & Nesbet R K 1984 *Comput. Phys. Commun.* **33**, 399.
- Osmann G, Bunker P R, Kraemer W P & Jensen P 1999 *Chem. Phys. Lett.* **309**, 299.
- Pople J A & Curtiss L A 1987 *J. Phys. Chem* **91**, 155.
- Pritchard B P, Altarawy D, Didier B, Gibson T D & Windus T L 2019 *J. Chem. Inf. Model.* **59**, 4814.
- Puglisi A, Miteva T, and J Paul Mosnier E T K, Bizau J M, Cubaynes D, Sisourat N & Carniato S 2018 *Phys. Chem. Chem. Phys.* **20**, 4415.
- Rabadán I & Tennyson J 1996 *J. Phys. B: At. Mol. Opt. Phys.* **29**, 3747–61.
- Reiter D & Janev R K 2010 *Contrib. Plasma Phys.* **50**, 986.
- Römel't J & Peyerimhoff D 1981 *Chem. Phys.* **54**, 147.
- Rösslein M, Gabrys C M, Jagod K F & Oka T 1992 *J. Mol. Spectrosc.* **153**, 738.
- Sarpal B K, Branchett S E, Tennyson J & Morgan L A 1991 *J. Phys. B: At. Mol. Opt. Phys.* **24**, 3685–99.
- Tennyson J 1996 *J. Phys. B: At. Mol. Opt. Phys.* **29** 1817–28.
- Tennyson J 2010 *Phys. Rep.* **491**, 29–76.
- Tennyson J & Noble C J 1984 *Comput. Phys. Commun.* **33**, 421.
- Tennyson J & Sutcliffe B T 1983 *J. Mol. Spectrosc.* **101**, 71.
- Theodorakopoulos G & Petsalakis I D 1991 *J. Molec. Struct. (THEOCHEM)* **230**, 205.
- van Dishoeck E F, Bearda R A & van Hemert M C 1996 *Astron. Astrophys.* **307**, 645.
- van Dishoeck E F, Jonkheid E F & van Hemert M C 2006 *Faraday Discuss.* **133**, 231.
- Vane C R, Bahati E M, Bannister M E & Thomas R D 2007 *Phys. Rev. A* **75**, 052715.
- Wakelam V, Smith I W M, Herbst E, Troe J, Geppert W, Linnartz H, K. Öberg, Roueff E, Agúndez

1
2
3 *e-CH₂⁺ collisions*

13

- 4
5 M, Pernot P, Cuppen H M, Loison J C & Talbi D 2010 *Space Sci. Rev.* **156**, 13.
6 Wang H, Neese C F, Morong C P, Kleshcheva M & Oka T 2013 *J. Phys. Chem.* **117**, 9908.
7 Willitsch S & Merkt F 2003 *J. Chem. Phys.* **118**, 2235.
8 Yamaguchi Y & Shaeffer III H F 1997 *J. Chem. Phys.* **106**, 1819.
9 Zhang R, Baluja K L, Franz J & Tennyson J 2011 *J. Phys. B: At. Mol. Opt. Phys.* **44**, 035203.
10
11
12
13
14
15
16
17
18
19
20
21
22
23
24
25
26
27
28
29
30
31
32
33
34
35
36
37
38
39
40
41
42
43
44
45
46
47
48
49
50
51
52
53
54
55
56
57
58
59
60

Accepted Manuscript